Title
INITIAL CHARACTERIZATION OF A MULTI-WIRE PROPORTIONAL CHAMBER POSITRON CAMERA

Authors
Lim, C.B.
Chu, D.
Kaufman, L.
et al.

Publication Date
1974-12-01

Presented at the IEEE Nuclear Science Symposium, Washington, D.C., December 11-13, 1974.

LBL-3617

INITIAL CHARACTERIZATION OF A MULTI-WIRE PROPORTIONAL CHAMBER POSITRON CAMERA

C. B. Lim, D. Chu, L. Kaufman,
V. Perez-Mendez, R. Hattner and D. C. Price

December 1974

Prepared for the U. S. Atomic Energy Commission under Contract W-7405-ENG-48

INITIAL CHARACTERIZATION OF A MULTI-WIRE PROPORTIONAL CHAMBER POSITRON CAMERA

C. B. Lim*, D. Chu†, L. Kaufman*, V. Perez-Mendez*†, R. Hattner* and D. C. Price*

University of California Medical School*

San Francisco, Ca.

and

Lawrence Berkeley Laboratory, Berkeley, Ca.†

Initial results of a research and development effort on a positron camera utilizing 48 x 48 cm^2 multi-wire proportional chambers for detecting the annihilation photons that follow positron decay are described. These photons are detected in the chambers by the photons' interaction with specially configured lead converters placed in close proximity to the chamber wire planes, and the coordinates of the interactions are localized by delay line electronics. A spatial resolution of 6 mm FWHM and a resolving time width of 350 nanoseconds have been achieved. Present sensitivity is of the order of 675 counts/min-μCi, with a maximum data rate of 20K counts/min. Scattering medium in the field of view does not significantly degrade performance. Initial in vivo images demonstrate the potential of this camera.

Introduction

Positron emitters offer a number of advantages for imaging in nuclear medicine. Their useful characteristics for imaging are that the annihilation of the positron produces a monochromatic 511 keV spectrum and detector parameters can be optimized for this energy. Because the annihilation photons are emitted at 180 deg to each other, collimators are unnecessary to determine activity distributions if the paired photons are detected in coincidence.

A number of positron-emitters are of special interest for diagnostic and kinetic studies. The only feasible imaging tracers for three of the most abundant components of biologic tissue, i.e., carbon, oxygen and nitrogen, are short lived positron emitters. With the increasing availability of accelerators in or near medical centers these tracers can be readily obtained, and positron cameras become an attractive adjunct to conventional imaging instrumentation.

Because positron emitters tend to be relatively short lived and accelerator produced, isotope costs are high. A notable exception is Ga-68, which can be obtained from an inexpensive 280 day half-life Ge-68 generator. Since Ga-68 is an almost pure positron-emitter with $T_{1/2}$ = 68 min and manageable chemistry, it offers considerable potential for nuclear medicine. Other isotopes of interest are Cu-64, a reactor produced $T_{1/2}$ = 12.8 hr isotope with potential for labeling the tumor-specific agent bleomycin; F-18, a cyclotron produced and commercially available $T_{1/2}$ = 110 min bone-seeker that may also localize in infarcted muscle and has good chemical characteristics for labeling organic compounds; and Rb-82, a potassium analogue with $T_{1/2}$ = 1.3 min that can be obtained from a 25 day half-life Sr-82 generator.

A number of cameras for positron-imaging in the coincidence mode have been developed. A system using two scintillation devices as detectors[1] was constructed and has been commercially available. Another approach uses two arrays of sodium-iodide crystals.[2] The presently reported positron-camera uses multi-wire proportional chambers (MWPC's) as detectors. (A smaller camera of this kind has been developed concurrently at the University of Alberta.[3]) The use of wire-chambers had suggested itself as advantageous at an early stage of development.[4] These detectors were chosen because they provide the following attractive characteristics:

1. Feasibility of large area detectors at low cost
2. Excellent spatial resolution
3. Good uniformity of response
4. Adequate timing resolution and dead-time
5. Low system cost

The disadvantages are:

1. Suboptimal detection efficiency
2. No energy resolution

The latter relative drawbacks are offset by both the favorable characteristics of the detectors and by the ideal matching of these detectors to physical processes involved in positron imaging.

The Positron Camera

Figure 1 shows a schematic representation of the positron camera. Four MWPC's are used, two on each side of the object. Because the conversion efficiency for 511 keV gamma-rays in the chamber gas (a mixture of argon and methane at atmospheric pressure) is negligible, each MWPC is coupled to specially configured lead converters. Spatial coordinates are obtained by the delay-line method, and a small computer is used for data acquisition, processing and display. Figure 2 shows the complete system. The various components of the positron camera are discussed below:

1. Detectors

Four 48 x 48 cm^2 MWPC's, two on each side of the object, are used. The average separation between chambers is 56 cm, realizing a geometric acceptance of 28% for a point source at the center of the field of view. In the horizontal midplane, the geometric acceptance drops to 46% of maximum at the edge of an approximately circular region of 30 cm diameter. This loss is smaller for off-median planes.

The MWPC's are described in reference 5. Coordinate readout is effected by the delay line method.[6] With the present delay lines, dead-time is approximately 2 μsec. Delay lines under construction will decrease the dead-time to 1 μsec, with negligible change in MWPC intrinsic spatial resolution, which is presently about 3 mm.

2. Lead converters

To obtain adequate detection efficiencies, specially configured lead converters have been coupled to the MWPCs. The converters increase the surface area of the detector per unit volume. Converters that consist of four layers of a lead honeycomb are employed.[5] Each layer is electrically isolated from the other, and a drift field is applied between them to extract the ionization electrons produced by the conversion electron (Figure 3). A disadvantage of this approach is that, because of the varying distance from the cathode to the cell depth where ionization can be deposited, differing drift time results. This degrades time resolution even when using the 70% Argon and 30% Methane gas mixture which has optimal drift time.[7] On the other hand, these converters have the additional beneficial effect of improving spatial resolution by limiting the range of most conversion electrons to the cell size. Figure 4 shows the timing curve obtained between a single-converter MWPC and a NaI crystal. Notice the four distinct peaks from ionizations arising from each honeycomb layer. Note also that the conversion process involves a degradation of energy resolution, and voids the possibility for pulse-height analysis of detected events. Figure 5 shows the resolving time for the full operating system.

We have previously documented efficiencies of the order of 2.5% for a single converter.[5] Presently, each chamber is coupled to one converter, which should yield a detection efficiency of approximately 5% per side. An additional converter will shortly be added to each MWPC further improving efficiency. Since the detection process is symmetric, a conversion efficiency of approximately 10% on each side would be estimated, but because of the converter shielding effect and the multiple-interactions rejection-circuitry, the effective efficiency will be lower. In the present configuration, the average detection efficiency of each converter is 1.7%, and the efficiency on each side anticipated with the above changes will be of the order of 6.8%.

3. Electronics

The delay-line electronic readout package is a CAMAC version of previously discussed circuitry.[8] The two MWPC's on each side are operated in an anti-coincidence mode, to eliminate background from cosmic rays and multiple interactions, both of which produce simultaneous signals on both MWPC's. Pile-up rejection circuitry is used to eliminate event occurring within the dead time of a MWPC. The two pairs of MWPC's are operated in a coincidence mode, with a variable-width timing gate. Data is acquired in list mode on a PDP11/20 computer. Each stored event encodes the conversion coordinates as a pair of x,y coordinates for each side, and clock time. Events are transferred in groups of up to 3000 events to disk, where up to a total of 300,000 can be stored. Presently, the lack of a mass storage medium such as magnetic tape limits the maximum number of events that can be accumulated for a single study to this value. Image reconstruction from the data is effected by calculating the intersection of the detected vectors with either horizontal (tomographic) or vertical (axial) planes. Images can then be corrected for field uniformity. Digital processing software such as background subtraction, contrast and edge enhancement and smoothing will be obtained by modifying available DEC Gamma 11 software.[9]

Camera Performance

The following parameters can be defined in the detection of pure positron emitters by the MWPC positron camera:

The sensitivity S,

$$S = 2.22 \times 10^6 \, Ge^2 \text{ counts/min-}\mu\text{Ci} \quad \text{(Eq. 1)}$$

where G is the geometric acceptance (0.28 in this case) and e is the effective detection efficiency on each side of the imaging subject.

From equation 1 and response data for F-18 sources (which include the effects of attenuation by the 2.5 mm aluminum entrance windows on each MWPC), we find S = 675 counts/min-μCi, and an effective detection efficiency for each side of e = 3.4%. Figure 6 shows experimental results obtained by imaging a point source and by accepting as on-target all events within a 1 cm^2 region around the source, and as off-target all other detected events. The off-target events have a small contribution from accidentals (i.e., events produced by detection of two uncorrelated annihilation photons arising within the resolving time of the detector). This contribution is small, and is given by the expression:

$$A = 82.14 \, G^2e^2N^2 \, \tau \text{ counts/min.} \quad \text{(Eq. 2)}$$

where A is the accidentals rate, τ is the coincidence gate width in nanoseconds, and N is the source activity in μCi. For an activity of 30 μCi, the total count rate is approximately 20K counts/min, and the accidentals rate found from equation 2 is A = 1.8K counts/min. This is corroborated by measurements obtained where one pair of detectors are delayed by approximately 1 μsec with respect to the other pair. This accidentals rate is far below the off-target event-rate, which for a 30 μCi source-strength is 9K counts/min. The source of off-target events has not been defined. No doubt, multiple scattering in the windows and converters are contributing factors. In this case, pulse-pile up rejection electronics for each delay-line will be investigated as means of alleviating the problem. The total count rate shows a deviation from linearity in the region where dead-time effects due to the delay-lines and to data transfer rate limitations become apparent.

The effects of scattering material in the path of the annihilation photons have been investigated. Data are shown in figure 7. While the total count rate drops exponentially, as expected, the rate of on-target to total count rate drops more gradually. The energy resolution capabilities of a scintillation camera would not significantly improve this situation. This can be seen as follows: for 511 keV photons the major interaction mechanism in tissue is Compton scattering, which at this energy shows a high degree of forward peaking. At 511 keV, a 15% energy loss (which would be accepted by the usual scintillation camera pulse-height window) corresponds to scattering through 35 degrees. Thus, most scattered events are accepted by both the MWPC and scintillation positron cameras.

Using Cu-64 line sources ($E_{\beta+}$ = 656 keV), spatial resolution of 6 mm and 7 mm FWHM are found for sources embedded in 1.25 cm and 10 cm of lucite, respectively (Figure 8). Thus, scattering has relatively small effect on both signal-to-noise and spatial resolution, and the lack of energy resolution in the MWPC's does not significantly alter the performance of the system.

Early Imaging Experience

The following images obtained with the MWPC positron camera demonstrate the capabilities of the system (no field uniformity correction or digital processing have been performed on these images). Figure 9a shows the image of a 1.5 cm diameter Cu-64 ring. Figure 9b demonstrates two Cu-64 wire sources separated by 1 cm. Figure 10 shows on-and off-focus axial and tomographic views of two Cu-64 point-sources separated by 10 cm. Figure 11 shows tomographic reconstruction of the upper body of a dog labeled with F-18.

Conclusion

The MWPC positron camera is a low cost device with a sensitivity of 675 counts/min-μCi, a spatial resolution of 6-7 mm FWHM, and a maximum count-rate of 20K counts/min. Operation with a total of eight lead converters will approximately quadruple sensitivity, and modification of the delay-lines will reduce detector dead-time. Image processing techniques suitable for this camera are now being developed and extensive testing with animal models and humans has been initiated.

Acknowledgements

This work has been partially supported by grant RANN/IT/GI 35142 from the NSF, and by the US Atomic Energy Commission. Dr. Kaufman is the recipient of a Public Health Service Research Career Development Award number GM 70598 from the NIGMS.

References

1. Anger, HO, and Van Dyke, DC: Human Bone Marrow Distribution Shown in vivo by Iron-52 and the Positron Scintillation Camera. Science 144:1587, 1964.

2. Burnham, CA, and Brownell, GL: A Multi-crystal Positron Camera. IEEE Trans, Nuc Sci NS-19:201, 1972.

3. Reynolds, RA, Snyder, RE, and Overton, TR: A Multi-Wire Proportional Chamber Positron Camera: Initial Results. Phys Med Bio (to be published)

4. Kaufman, L, Perez-Mendez, V, and Wollenberg, H: Application of Digitized Readout Spark Chambers to Clinical Uses. UCID-3184, June 1968.

5. Lim, CB, Chu, D, Kaufman, L, Perez-Mendez, V and Sperinde, J: Characteristics of Multi-Wire Proportional Chambers for Positron Imaging. IEEE Trans Nuc Sci NS-21:85, 1973.

6. Grove, R, Perez-Mendez, V and Sperinde, J: Improved Delay-lines for Proportional Wire Chamber Readout. Nuc Inst & Methods 106:407, 1973.

7. English, WN and Hanna, GC: Grid Ionization Chamber Measurements of Electron Drift Velocities in Gas Mixtures. Canadian Jour Phys 31:768, 1953.

8. Kaufman, L, Perez-Mendez, V, Shames D and Stoker, G: A Multi-Wire Proportional Chamber for Nuclear Medicine Applications. IEEE Trans Nucl Sci NS-19: 169, 1972.

9. Gamma 11 software is a Nuclear Medicine package from the Digital Equipment Corporation, Maynard, Mass.

Figure Captions

Figure 1. Schematic configuration of the MWPC Positron Camera.

Figure 2. The MWPC Positron Camera. Left, detection system, Center, CAMAC coordinate processing electronics. Right, PDP 11/20 computer.

Figure 3. Schematic configuration of the lead converters, also showing the electric field lines. The incoming gamma-ray interacts with the lead, producing a conversion electron. This electron ionizes the gas in its path, and the ionization electrons are then drifted to the MWPC sensitive region by the electric field.

Figure 4. Timing curve between a one-converter MWPC and a NaI crystal. Note the four distinct peaks, each originating in one of the four honeycomb layers.

Figure 5. Resolving time of the MWPC Positron Camera.

Figure 6. Total and on-target count-rates as a function of source intensity. The rates arising from the detection of accidental coincidences are also shown.

Figure 7. Total and on-target/total count-rates as a function of absorber thickness in the path of the annihilation photons.

Figure 8. A. Cu-64 line source in 1.25 cm of lucite, showing a spatial resolution of 6 mm FWHM. B. Same source in 10 cm lucite. The resolution is 7 mm FWHM.

Figure 9. A. 1.5 cm diameter Cu-64 ring source. B. Two Cu-64 line sources separated by 1 cm.

Figure 10. Two point sources separated by 10 cm. Top: Axial reconstruction on the plane of the sources and two other planes separated by 1 cm. Bottom: Tomographic reconstruction on the planes of each source and on a plane half-way between them.

Figure 11. Images of F-18 in a dog reconstructed in planes separated by 2 cm from inferior to superior as indicated. Note the exquisite tomography with the mandible in focus at 2 cm, elbows at 6 cm, calvareal cavity and humeral heads at 8 cm, and cervical spine at 10 cm.

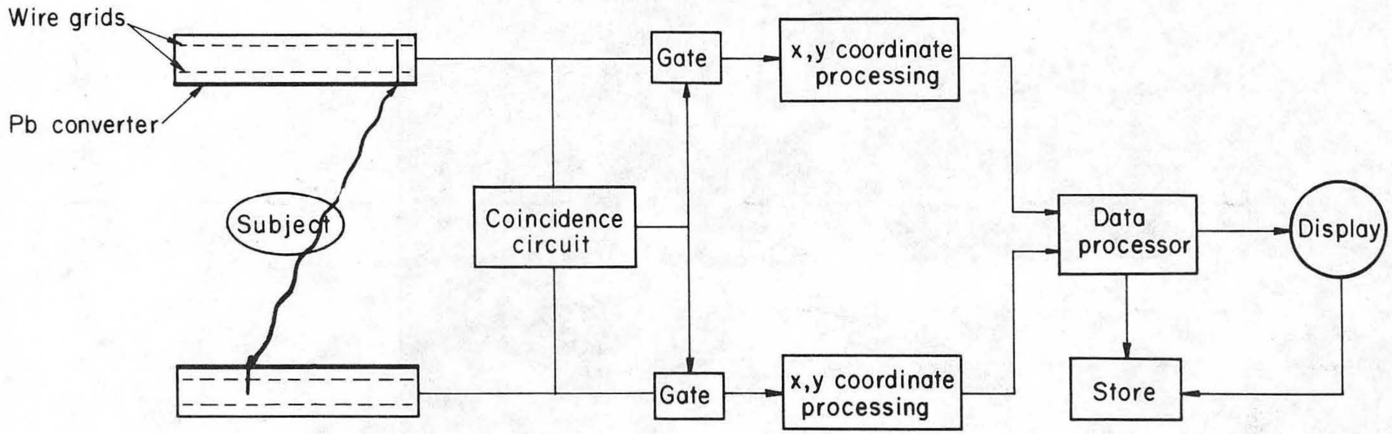

XBL708-3743

Figure 1

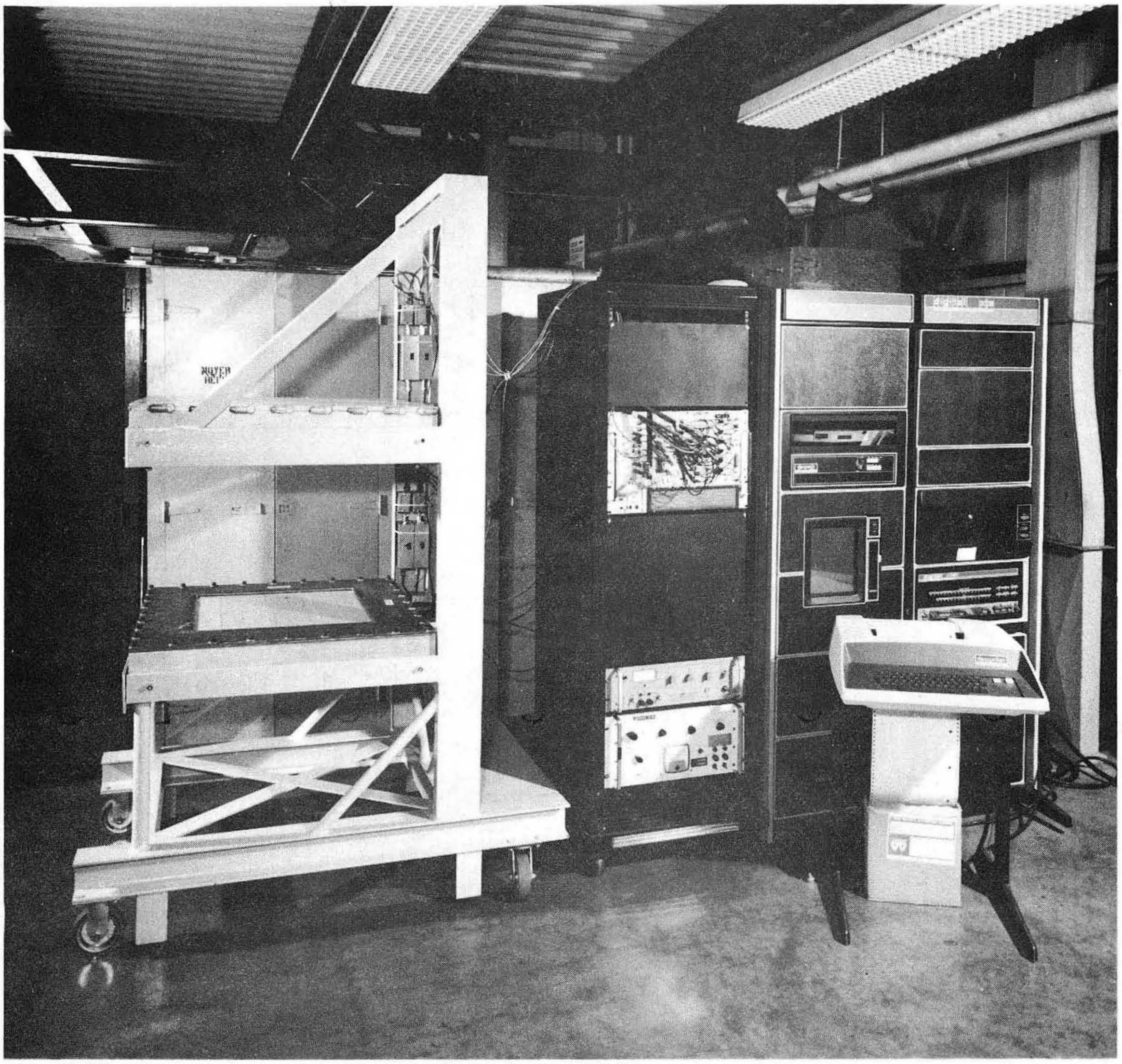

CBB 745-3643

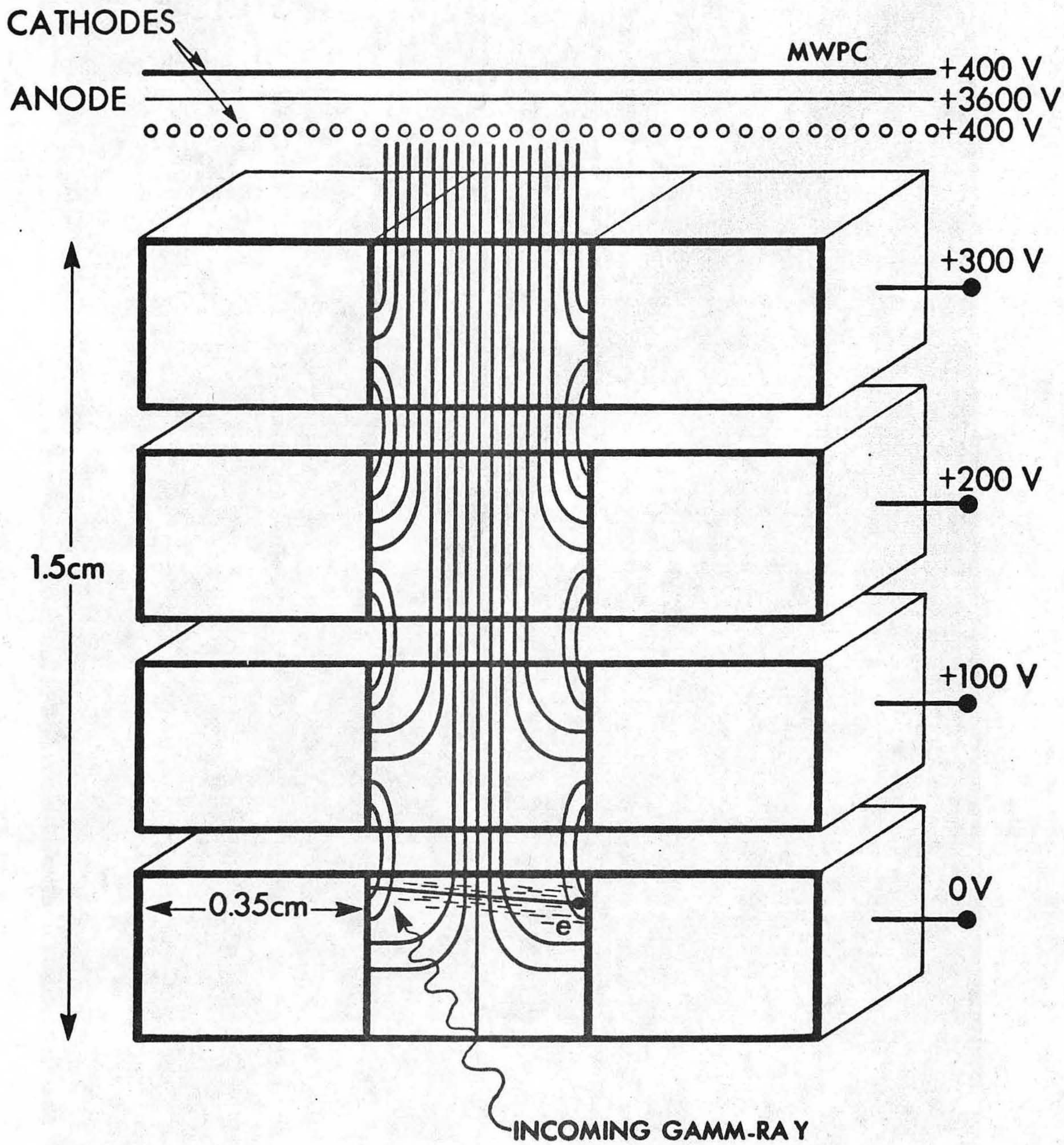

XBL 7411-8665

Figure 3

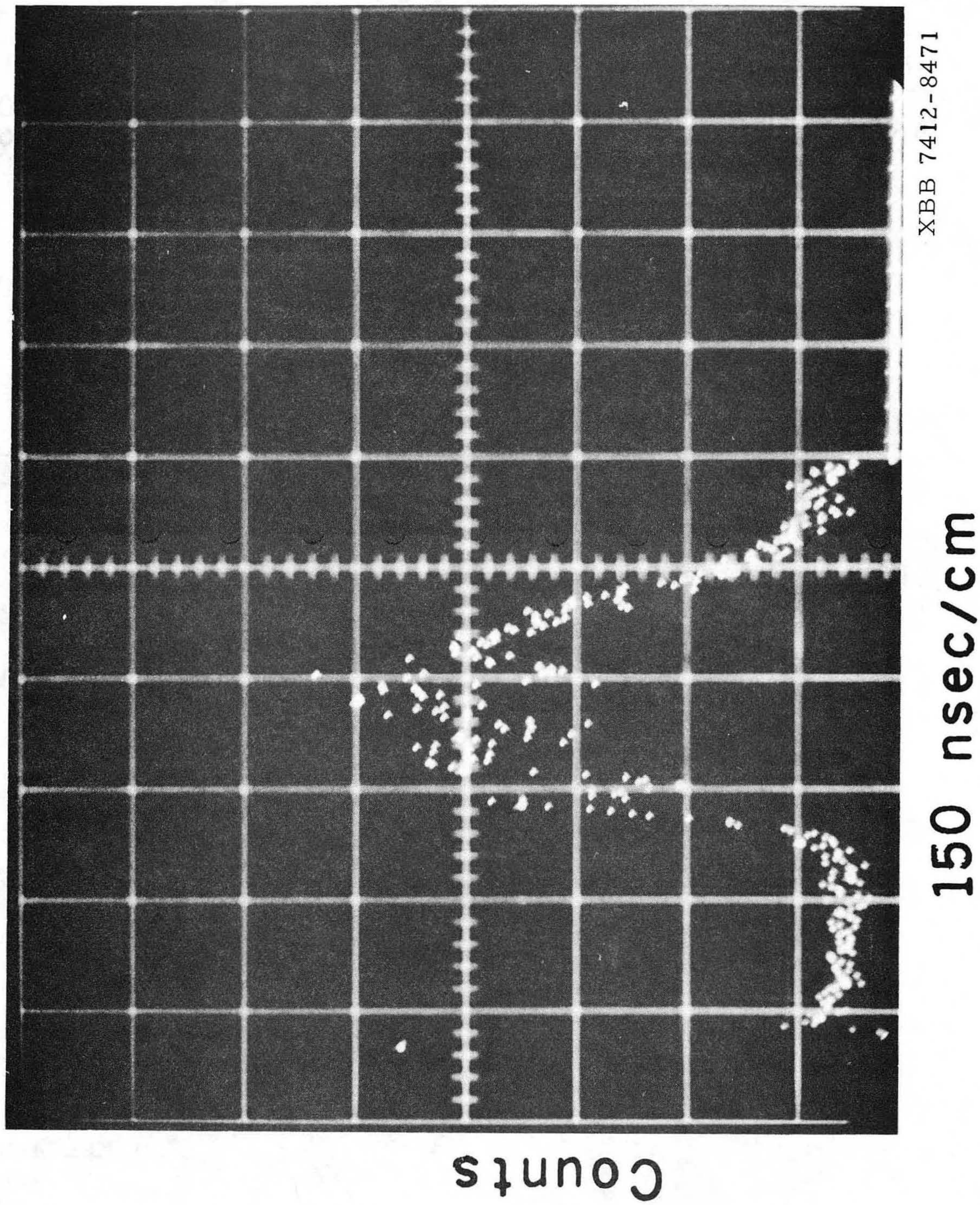

XBB 7412-8471

Figure 4

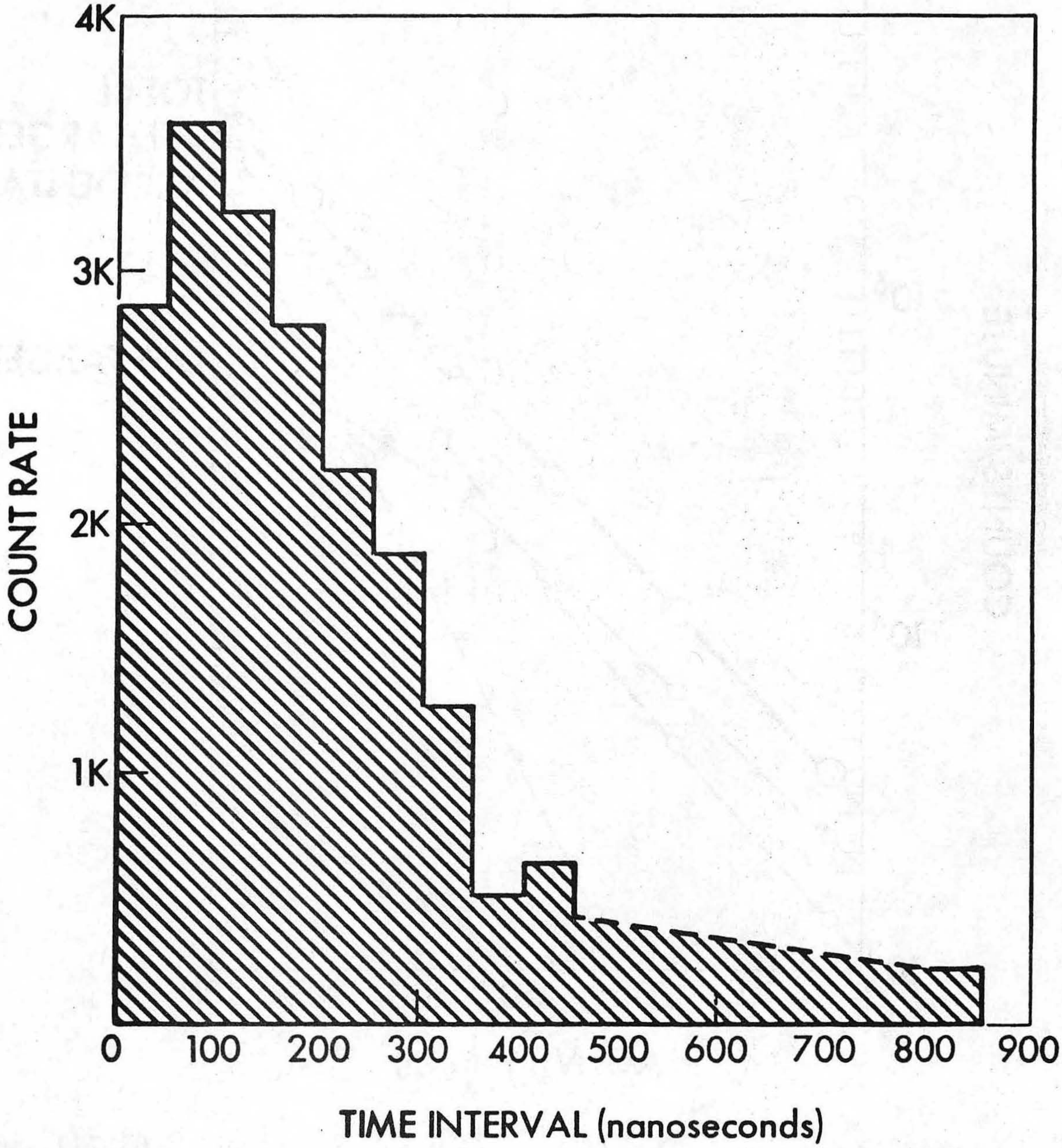

XBL 7411-8666

Figure 5

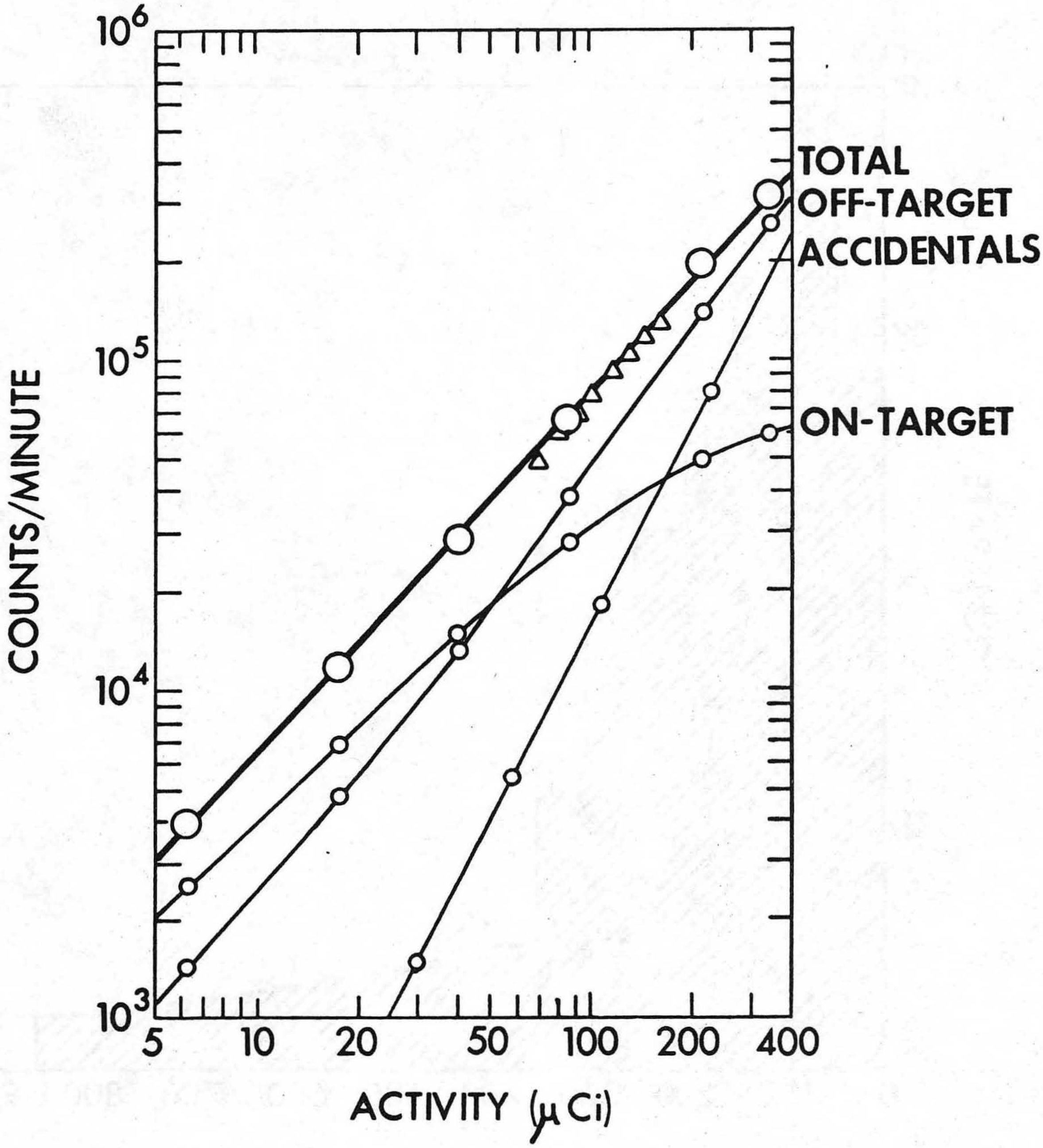

XBL 7411-8694

Figure 6

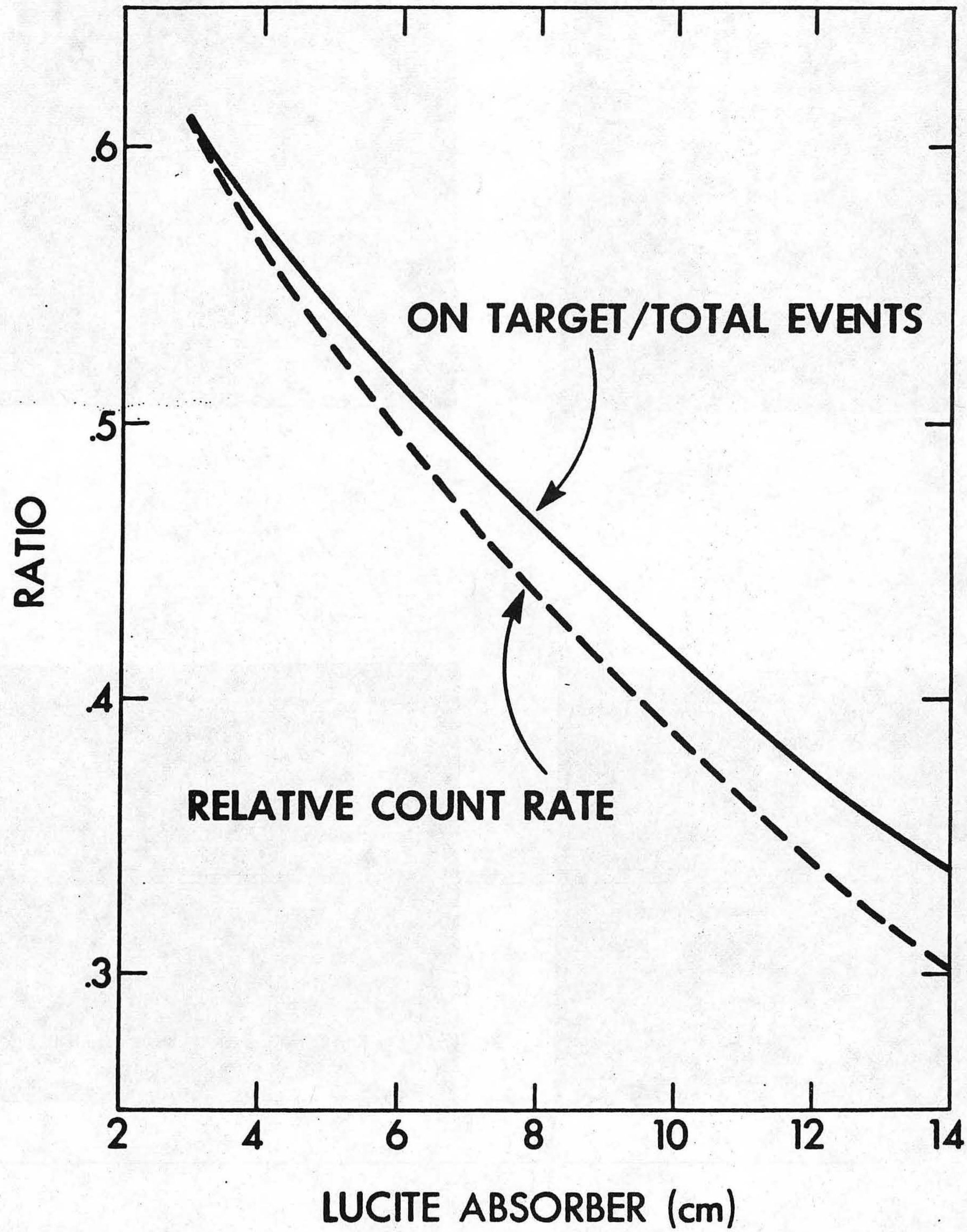

XBL 7411-8667

Figure 7

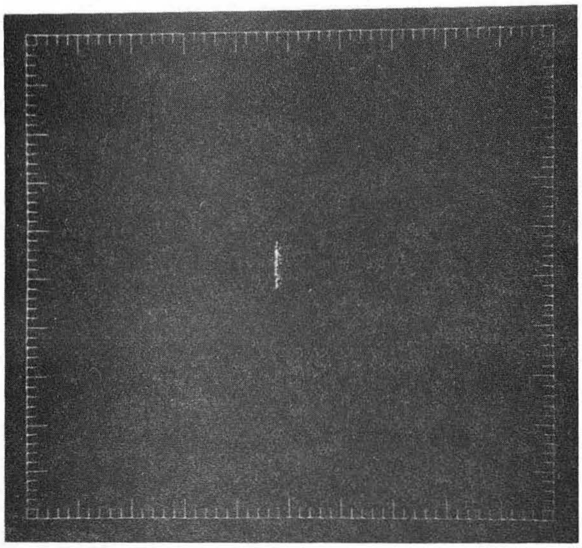

50 cm Full Scale

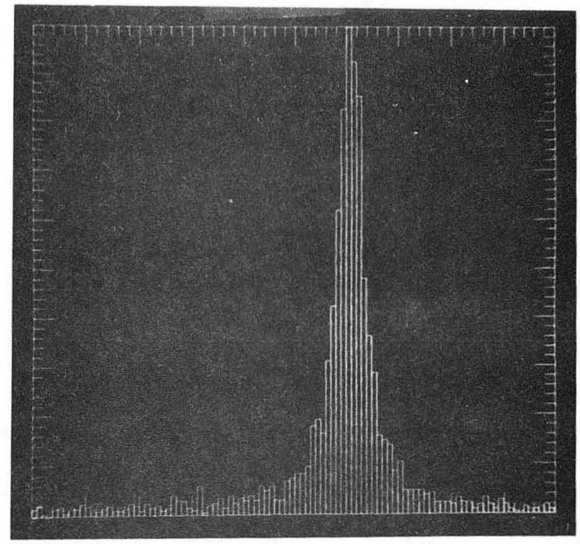

mm/bin

A

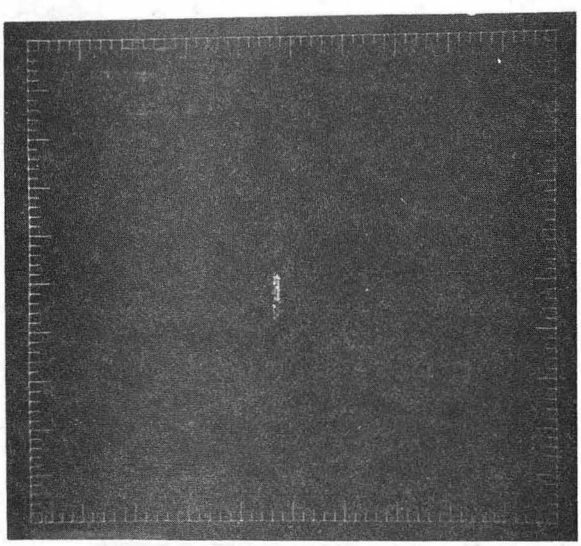

50 cm Full Scale

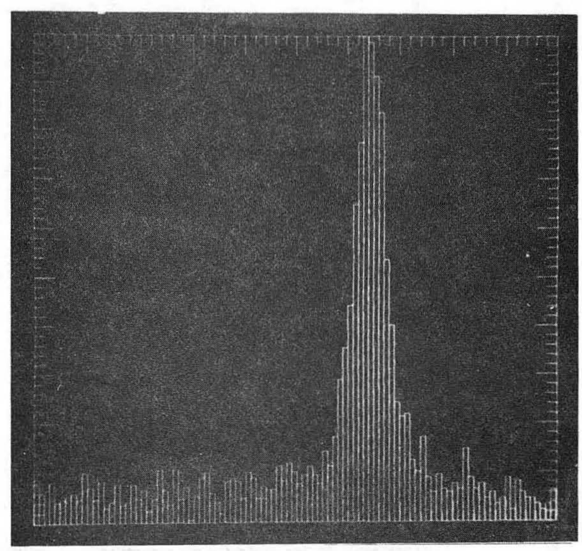

mm/bin

XBB 745-3590

B

Figure 8

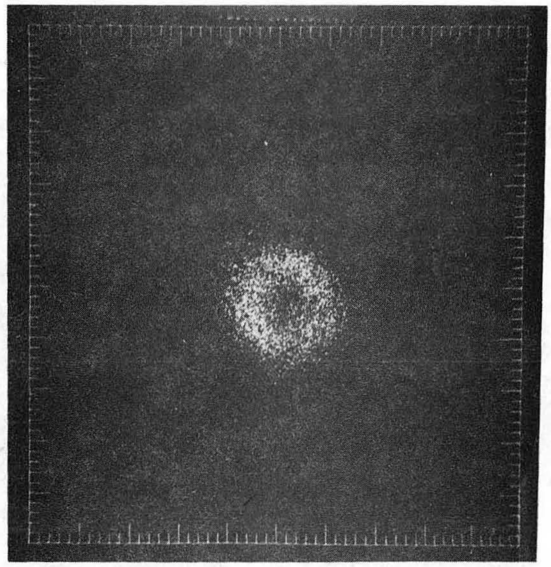

10 cm Full Scale

A

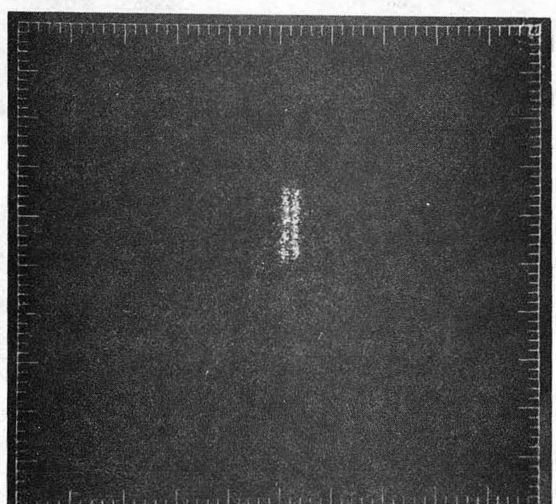

XBB 745-3591

50 cm Full Scale

B

Figure 9

AXIAL RECONSTRUCTION, TWO POINT SOURCES

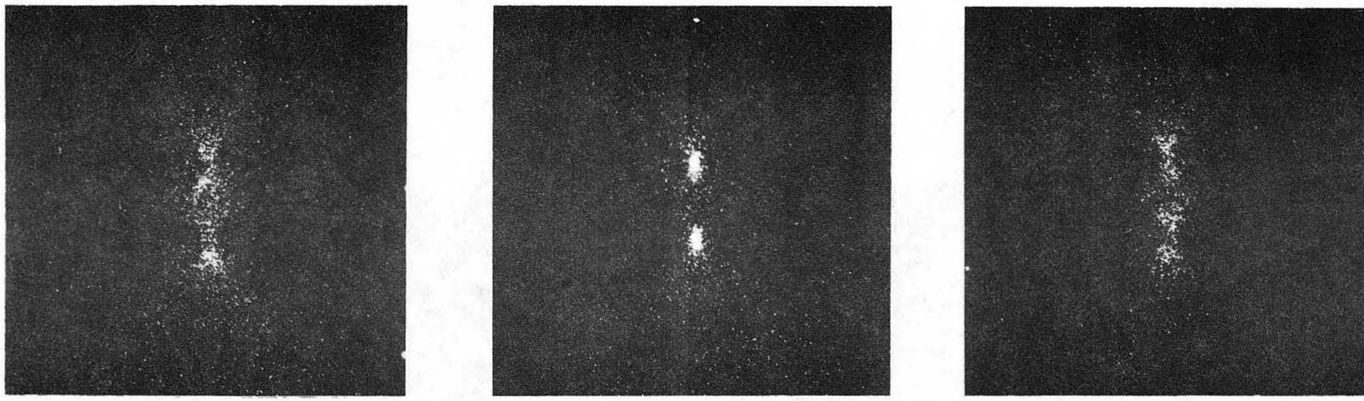

-1 cm　　0 cm　　+1cm

TOMOGRAPHIC RECONSTRUCTION

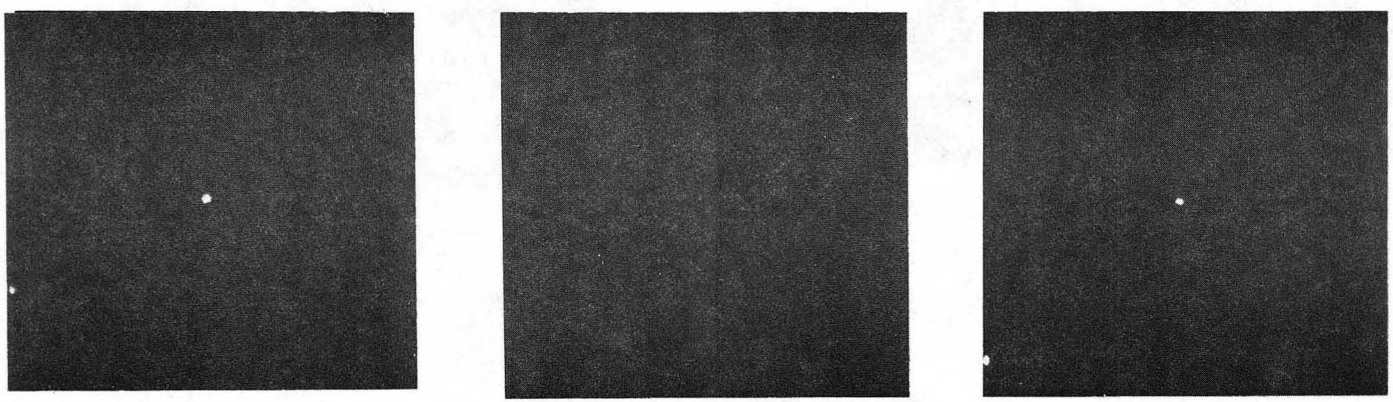

-5 cm　　0 cm　　+5 cm

XBB 7411-8284

Figure 10

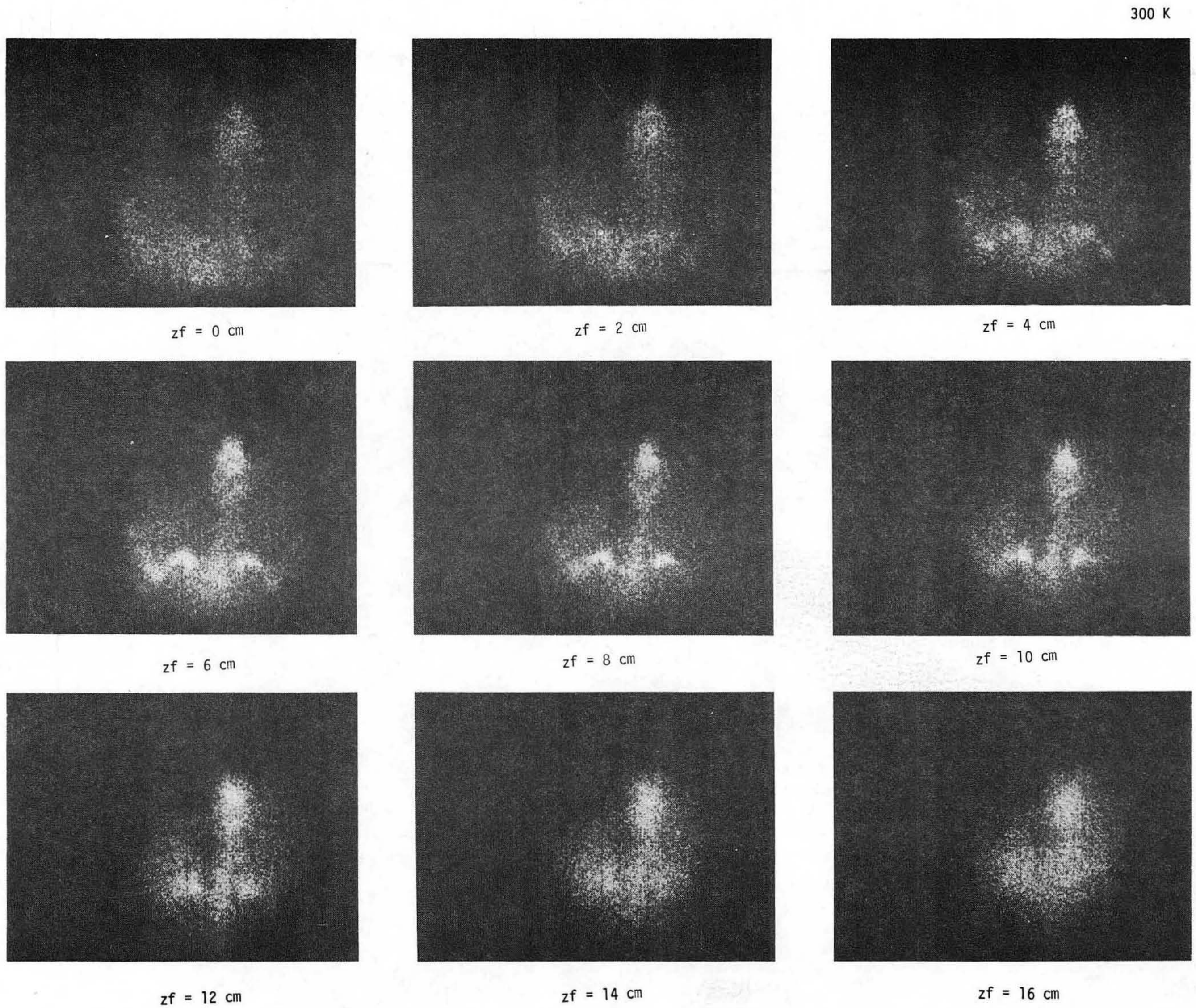

XBB 748-5311

Figure 11

LEGAL NOTICE